TABLE I
PARAMETERS FOR 3 dB KEMP *et al.* TYPE COUPLERS

3 section

Ripple, dB	C_1=C_3, dB	C_2, dB	W%	B
0.1	19.97 (16.09)	7.0 (1.64)	86 (101)	2.51 (3.03)
0.25	17.63 (14.0)	6.73 (1.44)	104 (123)	3.17 (4.18)
0.5	15.24 (11.82)	6.42 (1.21)	120 (141)	4.0 (5.81)
1.0	12.28 (8.95)	5.95 (0.89)	136 (161)	5.25 (9.20)

5 Section

Ripple, dB	C_1=C_5, dB	C_2=C_4, dB	C_3, dB	W%	B
0.1	23.1 (22.45)	13.67 (10.27)	6.24 (1.10)	116 (133)	3.76 (4.93)
0.25	19.6 (18.74)	12.13 (8.72)	5.98 (0.94)	130 (149)	4.71 (6.89)
0.5	16.3 (15.35)	10.65 (7.24)	5.70 (0.77)	142 (162)	5.90 (9.63)
1.0	12.5 (11.35)	8.88 (5.38)	5.30 (0.55)	153 (175)	7.51 (15.24)

7 Section

Ripple, dB	C_1=C_7, dB	C_2=C_6, dB	C_3=C_5, dB	C_4, dB	W%	B
0.1	25.2 (25.84)	15.8 (15.53)	10.55 (7.50)	5.71 (0.82)	134 (150)	5.06 (6.95)
0.25	20.85 (21.13)	13.53 (12.94)	9.42 (6.31)	5.47 (0.69)	146 (163)	6.41 (9.73)
0.5	17.16 (17.07)	11.48 (10.62)	8.36 (5.21)	5.22 (0.56)	154 (173)	7.70 (13.56)
1.0	12.9 (12.49)	9.1 (7.85)	7.1 (3.83)	4.85 (0.39)	162 (182)	9.53 (21.41)

$C_i = 10 \log_{10} k_i^2$

the reason is immediately evident from the even-mode network in Fig. 1(d).

An alternative method of achieving ultra-broad-band 3 dB quadrature couplers is to use either a discrete or a continuous tandem multisection construction [6], [7]. This technique would seem to have two distinct advantages over the Kemp approach; namely, the bandwidth contraction problem is eliminated, allowing decade bandwidths to be achieved, and the two couplers can be separated by an arbitrary amount to reduce cross-coupling without affecting the amplitude response because the interconnection occurs at the exterior rather than the interior ports (see the Appendix).

III. CONCLUSIONS

An analysis has been presented of the Kemp *et al.* type of 3 dB quadrature coupler, and a table of element values has been given. It has been shown that the Kemp approach overcomes the tight coupling problem associated with the Cristal and Young method but there is a severe bandwidth contraction penalty. It has also been shown that the use of interconnection lines sufficiently long to reduce cross-coupling causes an unacceptable degradation in coupling performance. Finally, although the technique provides a useful increase in bandwidth over that obtainable from a single-section coupler, it is suggested that the tandem multisection method is more suitable for decade bandwidths.

APPENDIX
DERIVATION OF EVEN-MODE EQUIVALENT CIRCUIT OF THE CENTRAL TANDEM SECTION

With reference to Fig. 2(b) one has

$$\begin{bmatrix} b_1 \\ b_2 \\ b_3 \\ b_4 \end{bmatrix} = \begin{bmatrix} 0 & S_{12} & S_{13} & 0 \\ S_{12} & 0 & 0 & S_{24} \\ S_{13} & 0 & 0 & S_{34} \\ 0 & S_{24} & S_{24} & 0 \end{bmatrix} \begin{bmatrix} a_1 \\ a_2 \\ a_3 \\ a_4 \end{bmatrix} \tag{A1}$$

with

$$a_2 = e^{-j\phi} b_2 \qquad a_3 = e^{-j\phi} b_3. \tag{A2}$$

Also, for the case considered here,

$$S_{24} = S_{13}, S_{34} = S_{12}. \tag{A3}$$

Substituting (A2) and (A3) into (A1) results in

$$\begin{pmatrix} b_1 \\ b_4 \end{pmatrix} = e^{-j\phi} \begin{pmatrix} S_{12}^2 + S_{13}^2 & 2S_{12}S_{13} \\ 2S_{12}S_{13} & S_{12}^2 + S_{13}^2 \end{pmatrix} \begin{pmatrix} a_1 \\ a_4 \end{pmatrix}. \tag{A4}$$

The equivalent circuit of Fig. 2(b) with $\phi = 0$ is known (see, for example, [5]) and (A4) shows that the effect of a nonzero value for ϕ is to introduce a unit element of length $\phi/2$ and characteristic impedance Z_0 at the input and output of the known circuit.

REFERENCES

[1] J. L. B. Walker, "Improving operation of classic broadband, balanced amplifiers," *Microwaves & RF* vol. 26, pp. 175–180, Sept. 1987.
[2] J. Lange, "Interdigitated stripline quadrature hybrid," *IEEE Trans. Microwave Theory Tech.*, vol. MTT-17, pp. 1150–1151, Dec. 1969.
[3] E. G. Cristal and L. Young, "Theory and tables of optimum symmetrical TEM-mode coupled transmission line directional couplers," *IEEE Trans. Microwave Theory Tech.*, vol. MTT-13, pp. 544–558, Sept. 1965
[4] G. Kemp, J. Hobdell, and J. W. Biggin, "Ultra-wideband quadrature coupler," *Electron Lett.*, vol. 19, pp. 197–199, Mar. 1983.
[5] R. J. Wenzel, "Exact design of TEM microwave networks using quarter-wave lines," *IEEE Trans. Microwave Theory Tech.*, vol. MTT-12, pp. 94–111, Jan. 1964.
[6] J. P. Shelton and J. A. Mosko, "Synthesis and design of wide-band equal-ripple TEM directional couplers and fixed phase shifters," *IEEE Trans. Microwave Theory Tech.*, vol. MTT-14, pp. 462–473, Oct. 1966.
[7] S. Uysal and A. H. Aghvami, "Synthesis and design of wideband symmetrical non-uniform directional couplers for MIC applications," in 1988 *IEEE MTT-S Int. Microwave Symp. Dig.* pp.587–590.

Percutaneous Transluminal Microwave Balloon Angioplasty

A. ROSEN, SENIOR MEMBER, IEEE, P. WALINSKY, D. SMITH, Y. SHI, Z. KOSMAN, A. MARTINEZ-HERNANDEZ, H. ROSEN, F. STERZER, FELLOW, IEEE, D. MAWHINNEY, MEMBER, IEEE, A. PRESSER, J.-S. CHOU, MEMBER, IEEE, P. GOTH, AND G. LOWERY

***Abstract*—Microwave balloon angioplasty (MBA) combines conventional balloon angioplasty techniques with microwave heating to help enlarge the lumen of narrowed arteries and reduce the occurrence of**

Manuscript received March 21, 1989; revised August 10, 1989.
A. Rosen, P. Walinsky, D. Smith, Y. Shi, Z. Kosman, A. Martinez-Hernandez, and H. Rosen are with Thomas Jefferson University, Philadelphia, PA.
F. Sterzer, D. Mawhinney, and A. Presser are with MMTC, Inc., Princeton, NJ.
J.-S. Chou, P. Goth, and G. Lowery are with the Edwards LIS Division, Baxter Healthcare Corporation, Irvine, CA.
IEEE Log Number 8931561.

restenosis. An apparatus for the delivery of MBA using 2450 MHz heating power is described. Using this apparatus, local arterial wall temperatures as high as 90°C were obtained during MBA on anesthetized rabbits. Tissue modification of the arterial walls due to simultaneous ballooning and heating was observed.

I. Introduction

Percutaneous transluminal balloon catheter angioplasty has become a popular alternative therapy to open heart surgery since it carries less risk and is less expensive than surgery. This method involves the insertion of a catheter, tipped by a deflated balloon, into the lumen of an artery partially occluded by plaque. The balloon is then inflated to enlarge the lumen and thus increase coronary blood flow.

In this paper, we describe a microwave balloon angioplasty (MBA) catheter and its *in vitro* and *in vivo* effects on arterial tissue. Microwave energy, producing heat at the end of a balloon angioplasty catheter, can cause softening of an arterial plaque prior to or during inflation of the balloon. This process may result in more effective and longer lasting dilatation of previously stenosed arteries. Furthermore, there is a thermal compression of the three layers of the artery. Such thermal compression has potentially beneficial effects, including a decrease in arterial elastic recoil [1], [2].

II. Microwave Delivery System and Initial *In Vitro* Results

The microwave system consists of a 2450 MHz signal generator (capable of delivering up to 50 W), a directional coupler, and two power meters to measure forward and reflected power. A thin flexible coaxial cable, 0.034 in. in diameter, fits within a conventional balloon angioplasty catheter and is terminated by a radiating antenna. The major physical constraint on both the antenna structure and the transmission line is the diameter of the catheter through-lumen. In addition, the radiation pattern from the antenna must be reasonably uniform and confined to the volume around the balloon. One class of microwave radiating structures that appears to be compatible with these requirements is the insulated asymmetrical dipole [3]. The radiated microwave heating power is generally confined to the region around the "gap" in the outer conductor of the coaxial line. At any specific frequency of operation, the heating pattern can be optimized by selection of the length of the shorted section and the width of the gap. The dielectric loading effects of the tissue and the balloon inflation fluid are other factors that affect the selection of the antenna dimensions, tending to substantially reduce both dimensions as compared to free-space conditions.

The microwave transmission line also must be of a diameter small enough and flexible enough to fit within, and be advanced through the catheter. As the diameter of a coaxial cable is decreased, the attenuation of the cable increases and the microwave power loss in the cable becomes larger. Although available coaxial cables can be and have been used for experimental work, special cables which optimize loss and mechanical flexibility are currently being developed for practical implementation of the technique. With an experimental 42-in.-long coaxial cable, suitable for installation in a standard angioplasty catheter, and an antenna of the type described above, return loss at a somewhat lower frequency was measured with the antenna immersed in various media as shown in Fig. 1. As demonstrated by the small amount of reflected power when the antenna is loaded by a crude tissue phantom, namely saline-soaked sponges, the coupling of microwave power into tissue can be reasonably efficient from this cable-antenna assembly.

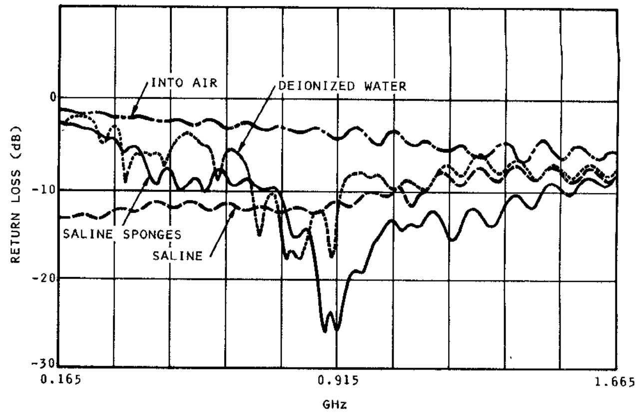

Fig. 1. Measured return loss

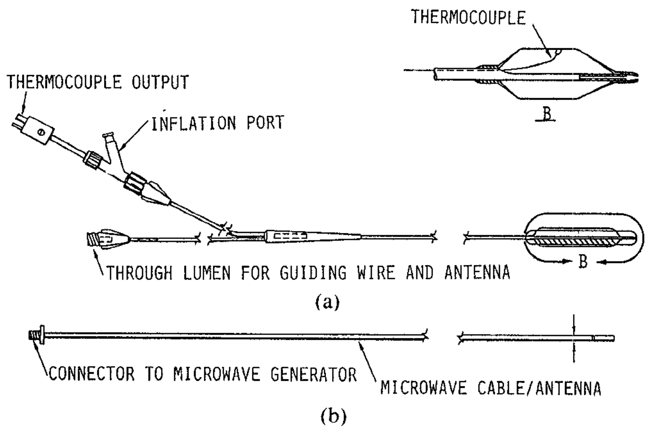

Fig. 2 (a) Balloon catheter. (b) Microwave delivery system.

A chromel/alumel (K type) thermocouple is inserted into a separate lumen of the catheter and epoxied to a portion of the balloon as shown in Fig. 2(a). The coaxial antenna is positioned within the balloon, and microwave energy is broadcast to surrounding arterial tissue. Fig. 2(b) depicts the microwave delivery system. The balloon catheter itself contains three lumens. The through lumen is the conduit for the guide wire and microwave antenna, while the other lumens are used for inflation of the balloon to a maximum of 3.5 mm and for insertion of the thermocouple.

The temperature increase and heating pattern of this slot antenna were measured by placing the antenna between two saline-soaked sponges. A liquid crystal sheet that changes color in the temperature range of 25–30°C was placed on the heated face of each sponge. The sponges were heated for 30 seconds with a net input power of 5 W at a frequency of 2450 MHz to measure temperature elevation. The heating pattern of the antenna was bidirectional and reasonably uniform over about 1 cm in length [4].

Having determined the heating properties of the antenna system, we applied microwave energy directly on top of the myocardium of a dog in an open chest experiment. No arrhythmia was observed. Fig. 3 depicts the histologic findings, consisting of a discrete area of tissue disruption, to a depth of 2–3 mm, which followed the application of microwave energy through a coaxial cable and radiating antenna. Centrally, the lesion contains a zone of severe thermal destruction with resulting coagulation necrosis. The extent of the coagulation necrosis gradually decreases towards the periphery of the lesion, where normal myocardial tissue is seen. The outer zones of tissue damage retain some connective tissue architecture despite the destruction of myocar-

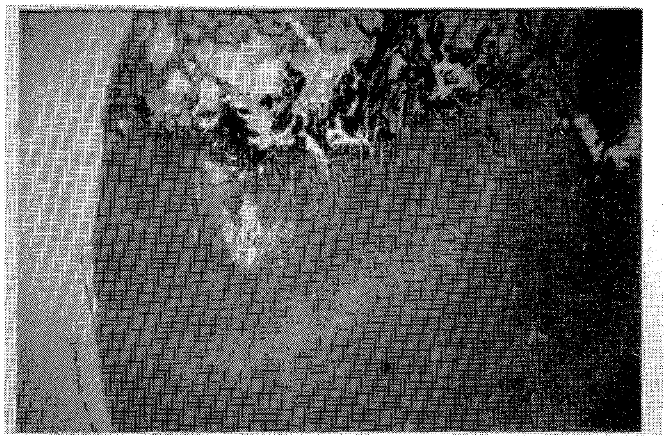

Fig. 3. Histological section of dog myocardium following thermal disruption by microwave energy.

dial tissue, and a few surviving fibroblasts are visible. These experiments, coupled with previous experience with microwave coaxial applicators for use in thermotherapy of brain tumors [5], suggest that sufficient energy can be introduced into the stenotic lumen of a coronary artery via a special microwave transmission line/antenna system embedded in a catheter. Such a system may be used to heat and potentially soften the plaque and, with the help of a balloon, to increase the flow through the lumen.

III. *In Vivo* Microwave Balloon Angioplasty on Rabbit Arterial Tissue

The MBA procedure is similar to a normal catheterization, where a catheter wire is guided through the artery to the site of the lesion. Studies were performed on New Zealand white rabbits, which were anesthetized with AcePromazine and Ketamine. The carotid artery was ligated and a balloon catheter was introduced into it. A guide wire (0.014 in.) was advanced through the balloon catheter and positioned in the iliac artery. The balloon catheter was advanced over the guide wire and positioned in the iliac artery (Fig. 4). Once the position of the balloon catheter was established, the guide wire was removed, and the same lumen was used to insert the coaxial microwave system. The antenna was positioned in the center of the balloon. The balloon was inflated at 2 atmospheres with deionized water for 15 seconds, and the microwave generator was then turned on. The deionized water and the balloon itself are relatively transparent to microwave energy, thus allowing for direct tissue volume heating to occur without significant loss of energy. Microwave power of between 10 and 15 W was delivered for 30–45 seconds, heating tissues to 70–90°C. Temperature was monitored by a thermocouple on the surface of the balloon adjacent to the gap antenna. At the end of power delivery, the balloon inflation was maintained for an additional 30 seconds, allowing the tissue to cool down. Deflation of the balloon immediately after the delivery of microwave power has resulted in balloon rupture.

The animals were sacrificed 3–5 hours after the microwave thermal balloon angioplasty. After fixation in formalin, H&E, trichrome, and VVG stains were performed. To date we have examined arteries from five animals exposed to different energy levels and sacrificed at different time intervals. Although the number of animals is too small to reach definitive conclusions, a pattern seems to emerge.

Histologic evaluation of the iliac arteries revealed injury to the intima and media. There appeared to be a correlation between the extent of injury and the peak temperature. The endothelium was denuded over a portion of the vessel. Coagulation necrosis of the smooth muscle was noted in the media. The depth of necrosis was variable. In the circumferential plane, the medial involvement was eccentric and not uniform. This relates to the eccentric position of the antenna within the inflated balloon. Although occasional changes were noted in the adventitia, the adventitia showed no major changes (Fig. 5).

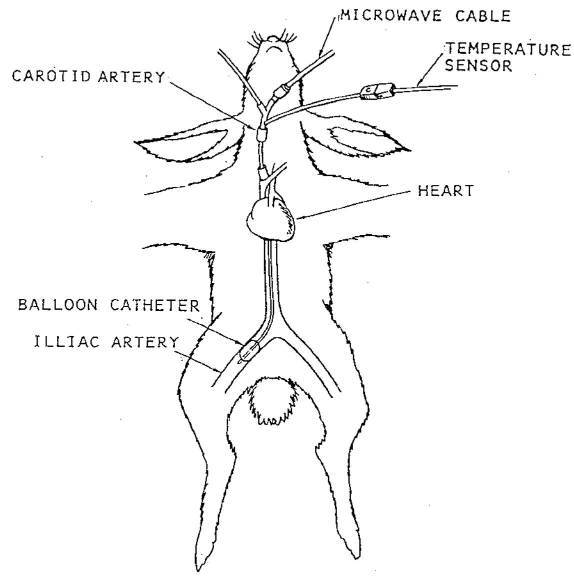

Fig. 4. Catheter inserted in rabbit model.

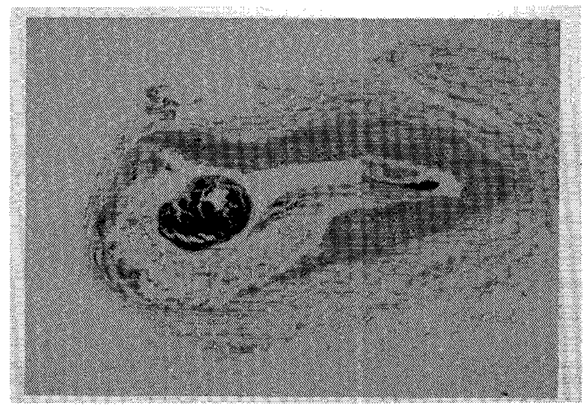

Fig. 5. Histological sections of rabbit illiac artery following *in vivo* microwave balloon angioplasty.

In order to verify the *in vivo* temperature measurements and the effect of the thermocouple wire on the measured temperature, *in vitro* measurements were conducted. In these experiments, an apparatus was prepared to hold a vessel with an inflated balloon microwave angioplasty catheter having one thermocouple attached to the inside of the balloon, and another in close proximity and at 90 degrees to it. The maximal variation in measured temperatures was found to be only 10 percent when the apparatus was immersed in normal saline solution. Such immersion simulates more closely the heat sink provided by body fluids in the *in vivo* experiments.

These studies demonstrate the feasibility of using ballooning combined with microwave heating to induce modification of vascular tissue. This modality is expected to have significant value in treating acute dissections, reducing arterial elastic recoil, forming a biological stent as demonstrated in *in vitro* experiments (Fig. 6), decreasing plaque resistance to dilatation, and reducing the incidence of restenosis.

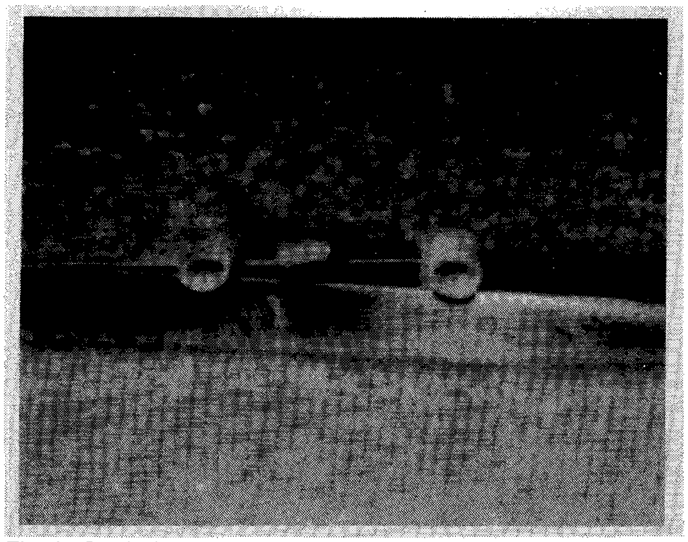

Fig. 6. Luminal view of rabbit artery before (center) and after (sides) *in vitro* balloon microwave angioplasty.

IV. Conclusion

Preliminary studies utilizing microwave balloon angioplasty at 2450 MHz were conducted. Local temperatures were raised to 90°C with a power of 15 W into the 0.032-in.-diameter coaxial cable, producing localized tissue modifications in both dog myocardium *in vitro* and rabbit arteries *in vivo*.

Acknowledgment

Special appreciation is due to D. T. Rosen for her invaluable contribution.

References

[1] A. Rosen and P. Walinsky, "Percutaneous transluminal microwave catheter angioplasty," U.S. Patent 4 643 186, Feb. 17, 1987.
[2] P. Walinsky, A. Rosen, and A. J. Greenspon, "Method and apparatus for high frequency ablation," U.S. Patent 4 641 649, Feb. 10, 1987.
[3] Y. Zhang, N. V. Dubal, R. Takemoto-Hambleton, and W. T. Joines, "The determination of the electromagnetic field and *SAR* pattern of an interstitial applicator in a dissipative dielectric medium," *IEEE Trans. Microwave Theory Tech.*, vol. 36, pp. 1438–1444, Oct. 1988.
[4] T. L. Borok, A. Winter, J. Laing, R. Paglione, F. Sterzer, I. Sinclair, and J. Plafker, "Microwave hyperthermia radiosensitized iridium-192 for recurrent brain malingnancy," *Medical Dosimetry*, vol. 13, pp. 29–36.
[5] A. Winter, J. Laing, R. Paglione, and F. Sterzer, "Microwave hyperthermia for brain tumors", *Neurosurgery*, vol. 17, no. 3, 1985.

A Rigorous Variational Formulation of an *H* Plane Slot-Coupled Tee Junction

B. N. DAS, N. V. S. NARASIMHA SARMA, AND A. CHAKRABORTY

***Abstract*—The paper presents a rigorous analysis for the determination of an exact equivalent network for the slot-coupled *H* plane Tee junction, taking the effect of wall thickness into account. A variational formulation is used for the determination of the parameters of the network. The parameters of the *S* matrix as well as coupling are evaluated from the exact equivalent network. Comparisons between theoretical and experimental results wherever available are presented.**

Manuscript received April 5, 1989; revised August 24, 1989.

The authors are with the Department of Electronics and Electrical Communication Engineering, Indian Institute of Technology, Kharagpur - 721 302 India.

IEEE Log Number 8931776.

I. Introduction

In the investigations of slot-coupled Tee junctions reported in the literature [1] using the variational method, no rigorous analysis of the effect of wall thickness has been presented and no attempt has been made to evaluate the S matrix of the junction.

In the present work, a variational formulation similar to that used by Oliner [2] for a radiating slot is used for the evaluation of network parameters of a slot-coupled Tee junction taking the effect of wall thickness into account. This formulation demands a knowledge of dyadic Green's functions in the primary and coupled guides, which are evaluated using the formulation available in the literature [3]–[5].

The coupling slot in a waveguide wall of finite thickness is represented as a section of transmission line. In the equivalent network, this transmission line is coupled to the primary and secondary guides by transformers whose turns ratios are also evaluated.

The equivalent network of the three-port junction is used for the evaluation of S parameters as well as coupling between the primary and secondary guides. A comparison between theoretical and experimental results on coupling is presented.

II. Analysis

Fig. 1(a) shows the slot-coupled Tee junction and the coordinate system. The equivalent circuit of the junction is presented in Fig. 2.

At the cross section $Y' = 0$ plane of the guide, the electric field is of the form

$$E_{\text{slot}} = \begin{cases} E_1 \cos\dfrac{\pi z'}{2L} & \begin{matrix} -L < z' < L \\ -W < x' < W \end{matrix} \\ 0 & \text{elsewhere.} \end{cases} \tag{1}$$

This electric field in the cross section is replaced by equivalent magnetic current. The admittance presented by the Tee arm at the secondary terminals of T_2 is obtained from the self reaction of this current with the magnetic field in the coupled guide.

Expressing the magnetic field in the coupled guide in terms of modal voltages V_{mn}^e and V_{mn}^m of the TE and TM modes, the admittance presented at the interface D is obtained as

$$Y_{2s} = \frac{\sum\limits_m \sum\limits_n \left[V_{mn}^{e^2} y_0^e + V_{mn}^{m^2} y_0^m \right]}{V_{10}^e \cdot V_{10}^e} \tag{2}$$

where V_{10}^e, the dominant mode modal voltage in the secondary guide, is given by

$$V_{10}^e = \oint E_{\text{slot}} \cdot e_{10}^e \, ds = \sqrt{\frac{2}{ab}} \frac{4W \dfrac{\pi}{2L} \cos\dfrac{\pi L}{b}}{\left(\dfrac{\pi}{2L}\right)^2 - \left(\dfrac{\pi}{b}\right)^2} E_1. \tag{3}$$

Y_0^e and Y_0^m are the wave admittances of TE and TM modes respectively and e_{10}^e is the dominant mode vector function.

The admittance presented at the primary of transformer T_2 is given by

$$Y_2 = Y_{2s} n_2^2 \tag{4}$$